Economically Attractive Features of Steady-State Neoclassical Reversed Field Pinch Equilibrium with Low Aspect Ratio

S. Shiina 1), Y. Yagi 1), H. Sugimoto 1), H. Ashida 1), Y. Hirano 1), H. Koguchi 1), H. Sakakita 1), M. Taguchi 2), Y. Nagamine 3), Y. Osanai 3), K. Saito 3), M. Watanabe 3), M. Aizawa 3)

1) National Institute of Advanced Industrial Science and Technology, Tsukuba, Japan
2) College of Industrial Technology, Nihon University, Narashino, Japan
3) Institute of Quantum Science, Nihon University, Chiyoda-ku, Tokyo, Japan

e-mail: shiina-s@aist.go.jp

Abstract Dominant plasma self-induced current equilibrium is achieved together with the high β for the steady-state neoclassical reversed field pinch (RFP) equilibrium with low aspect ratio by broadening the plasma pressure profile. The RF-driven current, when the safety factor is smaller than unity, is much less than the self-induced current, which dominates (96%) the toroidal current. This neoclassical RFP equilibrium has strong magnetic shear or a high-stability beta ($\beta_t = 63\%$) due to its hollow current profile. It is shown that the obtained equilibrium is close to the relaxed-equilibrium state with a minimum energy, and is also robust against microinstabilities. These attractive features allow the economical design of compact steady-state fusion power plants with low cost of electricity (*COE*).

1. Introduction

A low-aspect-ratio approach enhances the neoclassical viscosity or the bootstrap current in both the banana regime and Pfirsch-Schluter regime [1], and also has a potential to improve the plasma confinement due to the generation of a less stochastic core magnetic field in the RFP with a quasi-single helicity (QSH) state [2]. In this work, the steady-state neoclassical magnetohydrodynamic (MHD) equilibrium with a low aspect ratio, which is solved self-consistently considering the plasma self-induced parallel current and the rf-driven one, is investigated upon broadening the plasma pressure / temperature profile, the equilibrium obtained has a high magnetic shear due to its hollow current profile, which gives a high stability beta, and simultaneously a dominant plasma self-induced current, which allows for an easier approach to steady-state confinement compared to the "TITAN" RFP reactor with high aspect ratio [3]. We also show that the low-aspect-ratio RFP configuration is close to the relaxed-equilibrium state with a minimum energy, which is predicted by the extremum of the Lyapunov functional [4], and is also robust against microinstabilities. These attractive features allow the economical design of compact steady-state fusion power plants with low *COE*.

2. Plasma self-induced current

The flux surface averaged total toroidal current (I_p) in the MHD equilibrium is given by

$$I_p = -(1/2\pi)\int (dp/d\psi)(\langle B_p^2\rangle/\langle B^2\rangle)\,dV + (1/2\pi)\int G\,(\langle \boldsymbol{j}\cdot\boldsymbol{B}\rangle/\langle B^2\rangle)\langle 1/R^2\rangle\,dV, \qquad (1)$$

where V is the volume of the region enclosed by a flux surface, $G = RB_t$, B_t the toroidal magnetic field, G and pressure p are the functions of poloidal flux function ψ, $\langle X\rangle$ is the flux surface average of X, $\langle X\rangle = \int (X / B_p)dl / (dl / B_p)$, B_p is the poloidal magnetic field, and $B = (B_t^2 + B_p^2)^{1/2}$. The first term

represents the contribution of perpendicular current I_ϕ^{PRP}, namely, the toroidal component of the Pfirsch-Schluter (PS) current (I_ϕ^{PS}) and the diamagnetic current (I_ϕ^{DM}), which plays a substantial role in RFP plasma where $B_p \geq B_t$. The second term is from the parallel current, namely. the bootstrap current of the bulk plasma (I_ϕ^{BSb}) and the ohmic current (I_ϕ^{OH}). Note that I_ϕ^{BSb} depends on the plasma pressure and temperature profiles. We also consider the alpha-particle-induced bootstrap current ($I_\phi^{BS\alpha}$) due to the finite banana width effects of fusion-produced alpha particles. We define here the self-induced plasma current as I_ϕ^{SI} ($\equiv I_\phi^{PRP} + I_\phi^{BSb} + I_\phi^{BS\alpha}$). The bootstrap current I_ϕ^{BS} ($\equiv I_\phi^{BSb} + I_\phi^{BS\alpha}$) increases as the aspect ratio A decreases because I_ϕ^{BS} arises due to the increasing anisotropy in the electron pressure tensor or viscosity with lowering A. Accordingly, I_ϕ^{SI} is high in low-aspect-ratio RFPs. The toroidal current density is hereafter named by replacing I_ϕ with j_ϕ. The particle trajectory in the axisymmetric configuration is reduced to the conventional trapping condition of trapped particles in the region of $\varepsilon^{1/2} >> \delta_a^{1/3}$, $1 / B_{min} \geq \lambda \geq / B_{max}$ ($\equiv \lambda_c$), where ε is the inverse aspect ratio r / R_0, δ_a is the banana width of the trapped particles defined as $\delta_a \equiv 2q_0\, \rho_0/\kappa\, R_0$ with the safety factor at the magnetic axis q_0, the Larmor radius ρ_0 for species 'a', the cross-sectional elongation parameter κ, the major radius R_0, and $\lambda = (1 - v_{//}^2 / v^2) / B$, where $v_{//}$ is the parallel velocity, and B_{min} and B_{max} are the minimum and maximum of magnetic field along the magnetic line of force, respectively. In the region of $\varepsilon^{1/2} << \delta_a^{1/3}$, the finite banana width effect is shown to modify the conventional bootstrap current around the magnetic axis and reduces the trapping condition at the magnetic axis, $|v_{//}| / v < \delta_a^{1/3}$ and $e_a v_{//} < 0$ where e_a is a charge for species a, indicating that the fraction of trapped particles is increased owing to the finite banana width effect. The modification is significant for high-energy particles and changes the particle trajectory from the banana orbit to the potato one. We take into account the finite banana width effects around the magnetic axis by replacing the trapping boundary parameter λ_c ($\equiv 1 / B_{max}$) with λ_c^+ ($\equiv 1 / B_0$) for $e_a v_{//} > 0$ and λ_c^- [$\equiv (1 - \delta_a^{2/3}) / B_0$] for $e_a v_{//} < 0$. Then, the bulk parallel bootstrap current density is expressed as

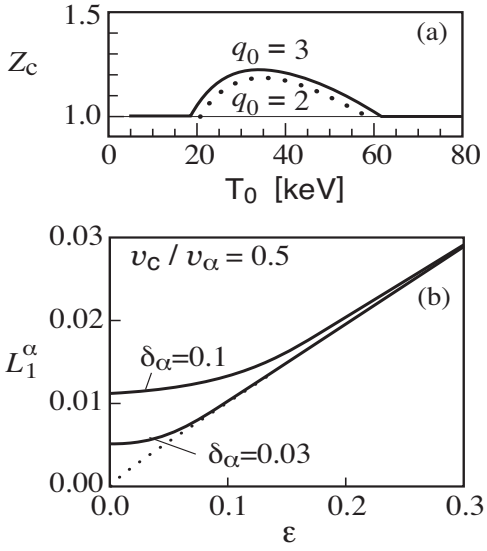

FIG 1. Critical effective ionic charge Z_c versus central temperature T_0 for central safety factor q_o (a), and transport coefficient L_1^α for Larmor radius with δ_α = 0.03 and δ_α = 0.1. The dotted line represents the conventional transport coefficient (b).

$$j_{bs}^{\,b} = (B^2 / \langle B^2 \rangle)\, (n_e\, T_e / B_p)\, j_{bs}^{\,b0},\; j_{bs}^{\,b0} = -\,L_1 \left[(p'_e / p_e) + (T_i / T_e)\, (p'_i / p_i) / Z \right] - L_2 (T'_e / T_e) - L_3\, (T'_i / T_e) / Z, \quad (2)$$

where n_a, T_a, and $p_a = n_a\, T_a$ are the number density, temperature, and pressure, respectively, Z is the effective ionic charge, L_k (k = 1, 2, 3) is the transport coefficient, and the prime denotes the differentiation with respect to the local minor radius r. The alpha-particle-induced parallel bootstrap current density is written as

$$j_{bs}^{\,\alpha} = (B^2 / \langle B^2 \rangle) [m_\alpha v_\alpha^{\,2}\, \tau_s\, dn_\alpha / dt] / 2B_p],\; j_{bs}^{\,\alpha 0} = -\,L_1^{\,\alpha}\, \partial \log(\tau_s\, dn_\alpha / dt) / \partial r + L_2^{\,\alpha}\, \partial \log (v_c^3) / \partial r, \quad (3)$$

where the subscript α denotes the value of the alpha particle, m_α is the mass, v_α is the initial velocity (3.5 MeV), dn_α / dt is the fusion production rate, τ_s is the slowing-down time and v_c is the critical

velocity defined as $(3\pi^{1/2}/4)\times\Sigma_j (m_e n_j e^2) \nu_e$ with Σ_j denoting a summation over only the ion species. The ratio of the critical velocity to v_α is estimated as $v_c/v_\alpha \sim 0.1\, T_e$[keV], and thus this ratio is on the order of unity for fusion plasmas. Therefore, the importance of retaining not only the slowing-down drag by electrons but also the pitch-angle scattering in the collision term is pointed out. $I_\phi^{BS\alpha}$ is accompanied by an electron return current due to the parallel momentum transfer from the alpha particles. The resulting net current density is written as $j^\alpha = j_{bs}^\alpha [1 - (Z_\alpha/Z)\, G]$, where $1 - (Z_\alpha/Z)\, G$ represents the shielding factor due to the electron return current, which therefore becomes zero on the axis at the critical effective charge number Z_c, which depends on q_0 and the central temperature T_0 (= $T_{e0} = T_{i0}$) [Fig. 1 (a)]. The parallel ohmic current density can be written as

$$j_{oh} = (e^2 n_e \tau_{ee}/m_e)\, L\, (\langle BE_{//}\rangle B/\langle B^2\rangle), \qquad (4)$$

where $\tau_{ee} = 3\,\pi^{1/2}/4\,\nu_{ee}$, ν_{ee} is the el-el collision frequency and $E_{//}$ is the parallel electric field. The transport coefficients L_k, L_k^α and L in the above equations are given in Ref. [5]. The coefficient L_k increases with lowering aspect ratio and increasing cross sectional ellipticity through the ratio of trapped particles to circulating ones. In this work, the finite banana width effect is considered only for L_k^α [Fig. 1 (b)], since it significantly modifies $I_\phi^{BS\alpha}$, while the expressions for L_k and L are approximated by conventional expressions. The transport coefficients L_1^α and L_2^α including the finite trapping ratio near the magnetic axis can be estimated by the j_{bs}^α expression mentioned above as $j_{bs}^\alpha = (1/2)[\, j_{bs}^\alpha(v_{//} > 0) + j_{bs}^\alpha(v_{//} < 0)]$ and by replacing λ_c with λ_c^+ for $v_{//} > 0$ and λ_c^- for $v_{//} < 0$ in the conventional theory. We calculate the thermal forces $\partial \log(\tau_s\, dn_\alpha/dt)/\partial r$ and $\partial \log(v_c^3)/\partial r$ in j_{bs}^α using an analytical fit for the deuterium-tritium (D-T) reaction rate. We find that the finite banana width effect strongly modifies the standard bootstrap current near the magnetic axis. In RFP with $q_0 < 1$, Z_c is expected to be smaller than 1.1, then j^α becomes positive value on the axis when $Z > 1.1$, and flows with a broad profile in the plasma column [Fig. 2 (c)].

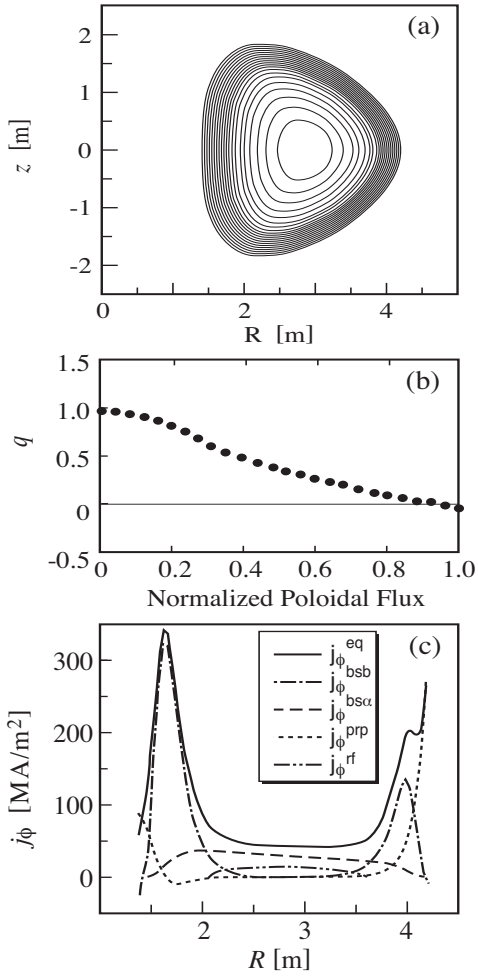

FIG. 2. Steady-state neoclassical RFP equilibrium. Magetic flux surface (a), profiles of safety factor, q, as a function of poloidal flux (b), and toroidal current density in midplane (c). Note that j_ϕ^{eq} has a hollow profile.

3. Target equilibrium and stability

The parallel currents, I_ϕ^{BSb}, $I_\phi^{BS\alpha}$ and I_ϕ^{OH} as well as the perpendicular current I_ϕ^{PRP} in RFP are self- consistently solved with the given initial functions $p(\psi)$ and $G(\psi)$ in order to simultaneously satisfy the Grad-Shafranov equation and the general MHD equation, using the formulae for the constituents of I_ϕ^{SI} as described above, and keeping the total toroidal current I_ϕ^{EQ} constant where $G(\psi)$ was solved iteratively until the summation of

$G(dG/d\psi)$ at all the flux surfaces converges with an accuracy on the order of 10^{-3}. Then, we obtain the neoclassical RFP equilibrium. First, we consider I_ϕ^{BSb}, I_ϕ^{OH} and I_ϕ^{PRP}. The result shows that I_ϕ^{BSb} has a hollow current profile with relatively broad plasma pressure and temperature profiles, namely, $p(\psi) = p_0 (1 - \psi_{00}^{bp})^{ap}$ and $T(\psi) = T_0(1 - \psi_{00}^{bt})^{at}$ [ψ_{00} is the normalized poloidal flux function; $\psi_{00} = (\psi - \psi_0) / (\psi_{lim} - \psi_0)$, $\psi_{lim} = 0$, $a_p = 1.0$, $b_p = 3.0$, $a_t = 0.75$ and $b_t = 3.0$] and the plasma parameters in TABLE I, where W_n ($= P_n / A_w$) is the neutron wall load for the total area of $A_w = 254 m^2$. The ratio of peak electron and ion temperatures is set at a value typical of power balance calculations for commercial plants, $T_{e0}/T_{i0} = 1.07$. I_ϕ^{EQ} consists of I_ϕ^{BSb} (62.32%), I_ϕ^{PRP} (22.38%) and I_ϕ^{OH} (14.53%). I_ϕ^{OH} has a broad profile, while I_ϕ^{PRP} flows near the boundary, and I_ϕ^{BSb} is localized just inside the reversal surface. The parallel currents, I_ϕ^{BSb} and I_ϕ^{OH}, dominate I_ϕ^{EQ}, namely, the force-free field is dominant (79.2%) inside the reversal surface. Hereafter, the toroidal current density j_ϕ is named by replacing I_ϕ with j_ϕ. The profile of the safety factor q has a strong magnetic shear due to the hollow current profile, which provides the toroidal β, with $\beta_t = 63\%$ stabilizing both the Mercier mode and the ideal kink mode, where $\beta_t = 2\mu_0 \langle p \rangle / B_t(0)^2$, in which $B_t(0)$ denotes the on-axis toroidal field and μ_0 denotes the vacuum permeability, and the poloidal β, with $\beta_p = 2\mu_0 \langle p \rangle / B_p(a)^2 = 45\%$.

TABLE I: DESIGN POINTS FOR ECONOMIC ANALYSIS

A	R_0	κ	β_t	q_0	B_0	I_ϕ^{eq}	$\langle n_e \rangle_{20}$	$\langle T_e \rangle$	$\langle T_i \rangle$	P_{CD}	P_E	W_n	M_{FPC}	MPD	Q_E	COE
	m		%		T	MA	m^{-3}	keV		MW	MWe	MW/m^2	kton	kWe/ton		mill/kWe•h
2	2.8	1.4	63	1.0	3.0	30.7	1.88	29.6	27.7	11.0	778	7.5	2.51	311	14.1	48.7

Next, the steady–state neoclassical RFP equilibrium without I_ϕ^{OH} is calculated by replacing I_ϕ^{OH} with $I_\phi^{BS\alpha}$ and the noninductive RF-driven current I_ϕ^{RF}. The good alignment of the plasma self-induced current profile with the profile of I_ϕ^{EQ} significantly lowers the requirements for the noninductive seed current. As shown in Fig. 2 (c), $I_\phi^{BS\alpha}$ has a broad profile, and is 17.42% of I_ϕ^{EQ} (= 30.72 MA) for the D-T-fueled plasma with $A = 2$, $R_0 = 2.8$ m, $\kappa = 1.4$, triangularity $\delta = 0.4$, $\delta_a = 0.05$ at $Z = 2.0$, and the central ion and electron temperatures $T_{i0} = 35$ keV and $T_{e0} = 37$ keV, respectively, considering the plasma power balance [6]. I_ϕ^{RF} is required to compensate for I_ϕ^{OH} in conjunction with $I_\phi^{BS\alpha}$, making q_0 smaller than unity. The required RF current is $I_\phi^{RF} \sim 1.18$ MA in the central region with the normalized poloidal flux function $\psi_{00} = 0 \sim 0.11$ ($\psi_{00} = 0$ at the magnetic axis) [TABLE II]. As a result, the current density has a hollow profile, that enhances the magnetic shear globally and locally [Fig. 2 (b)], then stabilizes both the ideal kink mode and Mercier mode at the toroidal beta value of $\beta_t = 63\%$. The greater part of I_ϕ^{EQ} is the parallel current with the fraction of 79.2%, which renders the force-free field dominant inside the reversal surface.

TABLE II: COMPOSITION OF TOROIDAL CURRENT IN STEADY-STATE NEOCLASSICAL RFP EQUILIBRIUM WITH $A = 2.0$ AND $\kappa/\delta = 1.4/0.4$.

I_ϕ^{EQ}[MA]	I_ϕ^{BSb}[MA]	$I_\phi^{BS\alpha}$[MA]	I_ϕ^{PRP}[MA]	I_ϕ^{RF}[MA]
30.72	17.8	5.35	6.39	1.18
100%	57.94%	17.42%	20.8%	3.84%

4. Features of minimum energy

The features of the minimum energy state for the low-aspect-ratio neoclassical equilibrium with a relatively broad plasma pressure profile might be explained by a minimum of the Lyapunov functional L, which is proposed as a condition for a minimum of energy and pressure and offers the possibility to find finite solutions with a significant maximum pressure at the center of the plasma [4, 7]. Their approach again uses the energy relaxation principle at a given constraint. This constraint is obtained in the frame of the conventional set of MHD equations:

$$M = \int h\, \mathrm{f}(p^{1/\gamma}/h)\, \mathrm{d}V = \text{const.} \tag{5}$$

Here h is the magnetic helicity $\boldsymbol{A}\cdot\boldsymbol{B}$ where $\boldsymbol{A}$ is the vector potential of the magnetic field $\boldsymbol{B}$, f(x) is an arbitrary function of its argument and γ is the adiabatic index. Under this more restrictive condition the plasma can relax to a state in which p has a significant maximum at the center of the plasma. In other words, a turbulent relaxation realizes a minimum of the Lyapunov functional $L = E + M$, where $E = \int[\rho v^2/2 + p/(\gamma\text{-}1) + B^2/2\mu_0]\mathrm{d}V$, ρ is the mass density, and $\boldsymbol{v}$ is the plasma velocity. When $p \to 0$ the function f (0) = const. and M is proportional to the total magnetic helicity K ($= \int h\mathrm{d}V$). But when p is not zero and f $\neq$ const., the variational principle of the extremum $\delta L = 0$ leads to the relaxed-equilibrium equation:

$$\nabla\times\boldsymbol{B} = -2H\boldsymbol{B} - \nabla H\times\mathbf{A}, H = H(h). \tag{6}$$

Here $H(h)$ is the function of h related to the f-function. It gives the steady-state pressure as a function of the helicity:

$$p\,(h) = \int h\,(\partial H/\partial h)\, \mathrm{d}h / \mu_0 + \text{const.} \tag{7}$$

The system of equations (6) and (7) singles out a very limited subset of the set of plasma equilibria. In the case of H = const., the current is parallel to $\boldsymbol{B}$ according to eq. (6), and there is a force-free state. The corresponding equation has been solved analytically by Taylor. We find other solutions of eq. (6) numerically in a cylindrical geometry with the coordinate system (r, θ, z). For this purpose we assume that all quantities depend on the cylindrical radius r alone. At $r = 0$, we set

$$A_z = \Psi, A_\theta = 0, B_z = 1, B_\theta = 0, (\nabla\times\boldsymbol{B})_z = 1, H = -1/2. \tag{8}$$

Here Ψ is a constant which, along H, determines the structure of the equilibrium. Conditions (8) introduce units of magnetic field and length, B_z and B_z / $(\nabla\times\boldsymbol{B})_z$, replacing at the magnetic axis. It is convenient to replace $H(h)$ by a function of r, such as $H = g(r) / 2$. Equation (7) then becomes

$$p(r) = \int_a^r h(\partial g / \partial r)\, \mathrm{d}r / 2\mu_0. \tag{9}$$

By specifying the values of g and Ψ, we can find the solutions of eq. (6) in the form of axisymmetric configurations. It is interesting to note that eq. (6) offers the possibility of finding finite solutions with zero current density near the plasma wall. Solutions of eq. (6) in the form of a reversed field pinch have been reported to have a high current density at the boundary [4].

Let us consider the solution of eq. (6) in the form of the neoclassical RFP equilibrium in which the plasma pressure has a relatively broad profile, namely, $p = p_0\,[1 - (r / a)^6]$ in a cylindrical geometric

approximation. At the axis we have $q_0 \sim 1$, and $h = \Psi (< 0)$ according to eq. (8). The ratio of the plasma pressure to the magnetic pressure at the axis is $\beta_0 = 0.84$, which is related to Ψ by

$$\beta_0 = \int_a^0 h(\partial g / \partial r)\mathrm{d}r = -\Psi - \int_a^0 (\partial h / \partial r) g \mathrm{d}r, \tag{10}$$

according to eq. (9), and increases with decreasing Ψ. The constant value of Ψ, which gives the helicity h at the axis, is determined in conjunction with β_0 by the profiles of $h(r)$ and $g(r)$ in the neoclassical equilibrium. The parallel current and the perpendicular current in the neoclassical equilibrium correspond to the first term (force-free current) and the second term (perpendicular current) considering the neoclassical effects in eq. (6), respectively. The second term leads mainly to the high current density at the boundary, where the contribution from the first term is negligibly small because of a weak toroidal field there. The toroidal current density at the boundary ($r = a$) is given by

$$j_z(a) \sim [(\partial g / \partial r) A_\theta]_{r=a} / 2\mu_0 \sim 3\beta_0 / \mu_0 \tag{11}$$

where $(\partial g / \partial r)_{r=a} = -2\mu_0 [(\partial p / \partial r) / h]_{r=a}$, $(A_\theta / h)_{r=a} \sim 1$, and $\beta_0 = 2\mu_0 p_0 / B_z^2(0)$ (= 0.84), using eq. (9). Note that $j_z(a)$ is higher by a factor of $3\beta_0$ than at the axis [see eq. (8)] indicating a hollow profile. The broader the pressure is near the axis, the larger the gradient $(\partial g / \partial r)_{r=a}$ becomes, and j_z thus is the larger at the boundary. It can be seen from eq. (9) that the $(\partial g / \partial r)$-profile has a larger spatial variation compared to the $(\partial p / \partial r)$-profile since the helicity h increases as the boundary is approached, and varies to a positive value ($\sim A_\theta$) at the boundary from a negative one (ψ) at the axis in the RFP.

In conclusion, the relaxed-equilibrium equation leads to a hollow profile of toroidal current density higher by factor $3\beta_0$ at the plasma boundary than at the axis, and thus is satisfied for the neoclassical RFP equilibrium with a broad plasma pressure profile. Considering the force-free current due to the increasing neoclassical effects with the decrease of the aspect ratio in the relaxed-equilibrium equation, the current profile becomes more hollow in the relaxed-equilibrium state as shown in Fig. 2 (c), indicating that the neoclassical RFP equilibrium is close to the relaxed-equilibrium state with a minimum energy.

In discussion, the high current density at the boundary is not altogether convenient for fusion purposes, but its existence and the presence of I_ϕ^{BSb} current flowing near the boundary would help external control to sustain the I_ϕ^{PRP} current if necessary, because the plasma reversal is not essentially affected by the increasing resistivity near the wall, and hence the steady state neoclassical RFP configuration having a broad pressure profile and a hollow current profile can be held with a dominant plasma self-induced current. It has been proposed to sustain and / or drive the current near the boundary to strengthen the magnetic shear there, in order to achieve the aim of weakening the dependence of stability on the conducting wall.

Even in MHD stable, dynamo-free RFPs, the energy confinement time might be determined by microinstabilities. The low-aspect-ratio RFP configuration has some favorable stability properties for microinstabilities. There exists a wide region of good curvature in a D-shaped cross section resulting in a high pitch magnetic line of force and strong paramagnetism. The on-axis maximum longitudinal adiabatic invariant ($J_{\max}$) or $\nabla p \cdot \nabla J > 0$ is attained in low-aspect-ratio RFPs with strong paramagnetism, which improves the stability of microinstabilities in the ion mode of trapped particles, the ion

temperature gradient (ITG) mode and probably the confinement degradation of high-energy particles due to the nonclosure magnetic field strength resulting from a small Shafranov shift in a tokamak with negative magnetic shear [8]. The toroidicity-induced Alfven eigenmodes (TAEs) are also reduced in RFP where the safety factor is small and B_p is strong at the plasma boundary. These attractive features allow the economical design of a compact steady-state fusion power plant with low *COE*.

5. Economical analysis

The compatibility of the dominant I_ϕ^{SI}, strong magnetic shear, and high β are economically attractive. This is because it significantly reduces the external current driving power required to generate the steady–state configuration and enhances the fusion power, thus lowering *COE* for fusion power plants [9]. The economic model using a simplified cost algorithm shows that the engineering power gain (Q_E; the ratio of plant gross electric power P_{ET} to circulation power P_C) and the mass power density (*MPD*; the ratio of net electric power P_E to the grid divided by the total mass of the fusion power core M_{FPC}) are the primary variables determining the *COE*. During the steady-state operation, part of P_{ET} is re-circulated for the RF current driving power (P_{CD}) and for maintaining the plant operation: $P_C = (P_{CD} / \eta_{CD}) + P_{PUMP} + P_{AUX}$; η_{CD} is the conversion efficiency of electric to RF power, P_{PUMP} is the partial recovery of coolant power (= 0.01 P_{ET}), and P_{AUX} is the auxiliary plant power (= 0.04 P_{ET}).

Using a low-frequency fast wave (LFFW; $\omega \sim 2\Omega_d$) providing the seed current in the core region with a high density / temperature, the requisite RF power (P_{CD}) is given by

$$I_\phi^{RF}[\mathrm{A}] / P_{CD}[\mathrm{W}] = (0.122 \langle T_e \rangle [\mathrm{keV}] / R_0[\mathrm{m}] \langle n_e \rangle_{20} [\mathrm{m}^{-3}]) \ln\Lambda \times j^* / p^*, \qquad (12)$$

where j^* / p^* is the normalized current drive efficiency and the function of parallel wave phase velocity normalized to the electron thermal velocity and lnΛ the Coulomb logarithm (~ 15), which depends on the current driving system only. The RF power spectrum is selected such that RFCD should create a current profile $G(\psi) = \langle \boldsymbol{j} \cdot \boldsymbol{B} \rangle_{RF} / \langle B^2 \rangle \sim \langle \boldsymbol{j} \cdot \boldsymbol{B} \rangle_{eq} / \langle B^2 \rangle - H(\psi)$, where $H(\psi)$ is the bootstrap current density. The value of j^* / p^* has been found to be 0.0175 from the RFCD in the dominant bootstrap current-aided reverse shear (RS) tokamak with a similar $G(\psi)$-profile using the same RF (low-frequency fast wave, LFFW; $\omega \sim 2\Omega_d$) current driving system [6]. Then the requisite RF power for I_ϕ^{RF} ~ 1.18 [MA] is evaluated to be P_{CD} = 11.0 [MW] for the D-T-fueled plasma. Our goal is to realize the steady-state compact power plant with a high *MPD* at high Q_E, namely, to realize the low *COE*. This goal is achieved for the neoclassical RFP equilibrium with a small P_C (= 59.6 MW), a low M_{FPC} (= 2.51×10^3 ton), and hence a high *MPD* (= 310 kWe / ton) with Q_E = 14.1, assuming η_{CD} = 62%. The constant *COE* contours are shown in Fig. 3. The low *COE* of 48.7 mill / kWe·h is attained with the other reactor characteristics in Table I, where P_n is the neutron power and W_n (= P_n / A_w) is the neutron wall load for the total area A_w of 254 m^2. The higher $\langle T_e \rangle$ at the given β_t results in the higher

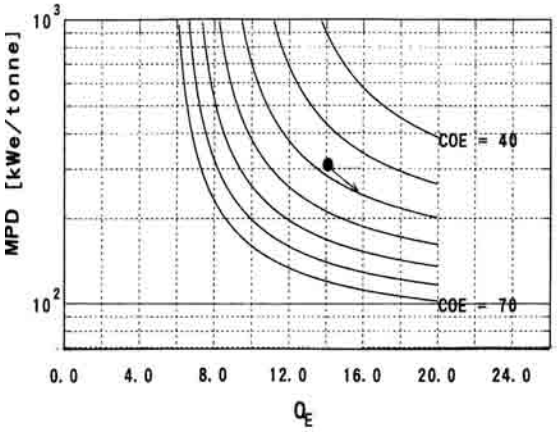

FIG. 3. COE for the steady-state neoclassical equilibrium with the design points in TABLE I.

Q_E (or the less P_{CD}) but the higher *COE*, as indicated by the arrow in Fig. 3.

6. Conclusion

The neoclassical equilibrium of a low-aspect-ratio RFP was studied in a reactor relevant parameter regime. There exists a compatibility between the high-stability beta (toroidal beta $\beta_t = 63\%$) and the dominant (96%) plasma self-induced current, which provides feasible steady-state RFP operation with high output power. The plasma pressure has a broad profile and the current density has a hollow profile, thus the magnetic shear is enhanced globally and locally. The equilibrium is close to the relaxed equilibrium with a minimum energy and is also robust against microinstabilities. These attractive features allow the economic design of compact steady-state fusion power plant with low *COE*.

An optimization study into the possibility of achieving the lower *COE* is desired, which varies the aspect ratio and the cross sectional shape such that they may further enhance the magnetic shear or the stability beta and the plasma self-induced current. There exist some different features between RFP neoclassical equilibrium and tokamak one. The strong paramagnetism would simplify the structure of a superconducting toroidal coil, rendering a lower aspect ratio possible. The present engineering techniques of the blanket and superconducting coil set the aspect ratio to $A \geq 2$ to attain the steady state reactor, which will make the transition from the first stability regime to the second one difficult because of the separation of each regime in the low-aspect-ratio tokamak, where the pressure-driven ballooning mode is the most dangerous and determines the stability beta limit keeping the current-driven kink mode stable [10]. On the other hand, the separation of the first and second stability regimes does not exist for the low- aspect-ratio RFP, where the stability beta limit is determined from the kink mode which can be stabilized by the globally negative magnetic shear. The neoclassical tearing modes, which are driven by the perturbed bootstrap current due to the pressure profile variation upon the appearance of magnetic island, are stabilized when $dp/dq > 0$, as in RFPs.

Acknowledgment
This work was financially supported by the Budget for Nuclear Research of the Ministry of Education, Culture, Sports, Science and Technology, based on screening and counseling by the Atomic Energy Commission.

References

[1] SHAING, K. C., et al., Phys. Plasmas **2** (1995) 349.
[2] MARTIN, P., 19th IAEA Fusion Energy Conf. (Lyon, 2002) IAEA-CN-94/EX/C1-2.
[3] KRAKOWSKI, R. A., "The TITAN RFP fusion reactor study", UCLA-PPG-1200 (1990).
[4] PETVIASHVILI, V. I., Sov. Phys. JETP Lett. **57** (1993) 103.
[5] TAGUCHI, M., J. Plasma Fusion Res. **77** (2001) 153.
[6] ERST, D. A., et al., Nucl. Fusion **38** (1998) 13.
[7] GORDIN, V. A. and PETVIASHVILI, V. I., JETP. **68** (1989) 988.
[8] FURUKAWA, M., J. Plasma Fusion Res. **74** (1998) 598.
[9] SHIINA, S., et al., to be published in J. Plasma Fusion Res. **6** (2004) P2-10.
[10] MILLER, R. L., et al., Phys. Plasmas **4** (1997) 1062.